

Synthesising Robust Controllers for Robot Collectives with Recurrent Tasks: A Case Study

Till Schnittka and Mario Gleirscher

University of Bremen, Germany

{schnittti,gleirsch}@uni-bremen.de

When designing correct-by-construction controllers for autonomous collectives, three key challenges are the task specification, the modelling, and its use at practical scale. In this paper, we focus on a simple yet useful abstraction for high-level controller synthesis for robot collectives with optimisation goals (e.g., maximum cleanliness, minimum energy consumption) and recurrence (e.g., re-establish contamination and charge thresholds) and safety (e.g., avoid full discharge, mutually exclusive room occupation) constraints. Due to technical limitations (related to scalability and using constraints in the synthesis), we simplify our graph-based setting from a stochastic two-player game into a single-player game on a partially observable Markov decision process (POMDP). Robustness against environmental uncertainty is encoded via partial observability. Linear-time correctness properties are verified separately after synthesising the POMDP strategy. We contribute at-scale guidance on POMDP modelling and controller synthesis for tasked robot collectives exemplified by the scenario of battery-driven robots responsible for cleaning public buildings with utilisation constraints.

1 Introduction

Hygiene in public buildings has been hotly debated ever since the increased safety requirements during the coronavirus pandemic. Autonomous robot collectives can help to relieve cleaning staff and keep highly frequented buildings (e.g., hospitals, schools) clean. However, commercially available solutions have their limitations, for example, a need for manual task programming or a lack of online adaptability. In contrast to domestic homes, there are strict regulations (e.g., [8] for schools) that stipulate which areas must be cleaned and at what intervals. Changing operational conditions (e.g., room occupation, equipment reconfiguration, cleaning profile, regulations) create the need for an automatic generation of cleaning schedules for robot collectives and for proving their compliance with hygiene requirements. This scenario is an instance of a multi-faceted *recurrent scheduling* problem discussed below.

Cleaning Buildings as a Running Example. When planning the cleaning of a building (e.g., a school), we can use its layout in the form of a room plan (Figure 1a). Apart from a set of m rooms $\mathcal{R} = \{\mathcal{R}_1, \dots, \mathcal{R}_m\}$ with an assigned area, such plans include the connections between rooms and the locations of n charging stations $C = \{C_1, \dots, C_n\}$. A collective of $k \leq n$ robots $B = \{B_1, \dots, B_k\}$ is responsible for cleaning \mathcal{R} . B is tasked to keep \mathcal{R} clean while charging its batteries using C . Each robot has a limited battery size and a charging point in C as an assigned resting position. Additionally, there is a room utilisation plan (Figure 1b) containing the times when the rooms are in use, which can change on a daily basis. While a room is in use, no cleaning robot may be inside and, thus, cannot clean it.

The task is to create a cleaning *strategy* (or schedule) for B , constrained by the utilisation plan and charging needs. Moreover, this strategy should keep the rooms clean enough, while minimising battery consumption. To specify this task adequately, we define cleanliness in terms of *contamination*. Since

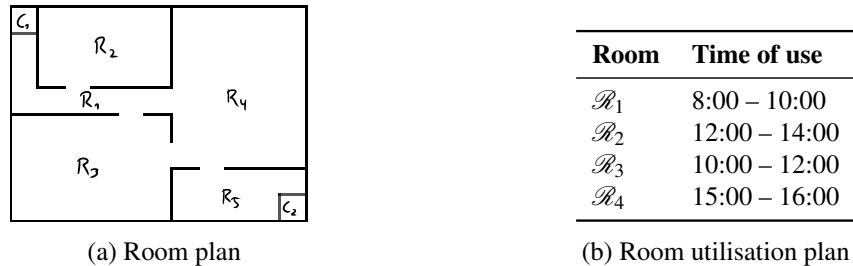


Figure 1: Examples of a room plan and the per-room utilisation

we are dealing with floor cleaning robots, we limit our definition to floor surfaces. For example, hygiene guidelines for schools [8] and the associated standard DIN 77400 [3] recommend cleaning intervals for floor surfaces. We reflect this recommendation in our definition by *contamination rates and thresholds*. Each room has a certain contamination rate. Over time, total contamination accumulates in a room and can be reset by cleaning. Clearly, the total contamination of a room should not exceed a certain threshold.

Approach. We propose a quantitative stochastic approach to synthesise strategies for robot collectives with recurrent tasks, such that the strategies are robustly (i.e., under uncertainty) compliant to recurrence and safety constraints and optimisation goals. We consider (i) weighted stochastic models and strategy synthesis for (ii) optimally coordinating robot collectives while (iii) providing guarantees (e.g., recurrence, safety) on the resulting strategies (iv) under uncertainty (e.g., partial observability). We select POMDPs, a generalisation of Markov decision processes (MDPs), for our problem.

Related Work. Among the works employing POMDPs for optimal planning, Macindoe et al. [11] show strategy synthesis for human-robot cooperative pursuit games with robots and humans acting in turns. Moreover, Thomas et al. [16] combine PDDL-based high-level task scheduling and POMDP-based low-level navigation. They use a Kalman filter to predict the distribution of the POMDP’s belief state based on discretised robot dynamics.

Using the PRISM model checker, Giaquinta et al. [4] show the synthesis of minimal-energy strategies for robots finding fixed objects. Object finding as an instance of navigation can be solved with memory-less strategies, that is, functions of the current state (here, positions of robot and object). Lacerda et al. [9] propose multi-objective synthesis of MDP policies satisfying *bounded co-safe LTL* properties using PRISM. Illustrated by a care robot, they employ a timed MDP and filter irrelevant transitions and states, resulting in a reduced MDP where time as a state variable preserves bounded properties. Basile et al. [2] use stochastic priced timed games and reinforcement learning (RL)-enhanced statistical model checking (with UPPAAL Stratego) to synthesise *safe, goal-reaching, and minimal-arrival-time* strategies for a *single* autonomous train operated under moving-block signalling.

El Mqirmi et al. [12] combine multi-agent RL and verification to coordinate robot collectives. An abstract MDP is generated from expert knowledge for optimal synthesis of a joint abstract strategy (using PRISM, STORM) under PCTL (safety) constraints. RL identifies a concrete strategy within these constraints by using shielding (i.e., only choosing actions compliant with the abstract strategy). Gu et al. [7] tackle state space reduction via RL to synthesise optimal navigation and task schedules for collectives (e.g., a quarry with autonomous vehicles) and timed games (in a UPPAAL Stratego extension) to check timed CTL properties (e.g., *liveness, safety, reachability*) of the synthesised strategies.

Vázquez et al. [17] developed a domain-specific language (DSL) for specifying tasks for collectives. Task allocation constraints are solved by ALLOY and plain MDPs are employed (via PRISM, EVOCHECKER) to synthesise *goal-reaching*, *minimum-travel-time* schedules.

Contributions. Our approach enhances works in optimal planning [11, 16] by a step of strategy verification against stochastic temporal properties. Object finding [4] corresponds to a *reachability* property, whereas continuous contamination and its removal to a *response* property. Moreover, object finding differs from *recurrent scheduling* in that it is static and can be realised with a simpler reward function and a smaller state space. Our problem involves a dynamic goal with robots operating 24 hours a day, having to coordinate their work continuously. Beyond bounded co-safe LTL [9], our approach supports *bounded response* properties $\mathbf{G}(\phi \rightarrow \mathbf{F}^{\leq T} \psi)$. The above works [9, 2, 12, 7] underpin the usefulness of stochastic abstractions for synthesis in various domains. Our use of POMDPs to hide parts of the stochastic process (e.g., contamination) and explicit concurrency (e.g., for many simultaneous robot movements) offers an alternative to obtaining small models for multi-agent synthesis under limited resources (e.g., time constraints to clean rooms). Additionally, we argue how the model of our case study—a collection of cleaning robots subjected to hygiene requirements—, while kept simple for illustrative purposes, scales and generalises to a range of similar scenarios in other application domains. Apart from our focus on recurrence and model reduction, a DSL [17] can wrap our approach into a practical workflow.

Overview. After giving key definitions in Section 2, we present our approach in Section 3. In the Sections 3.1 to 3.3, we explain the modelling, in Section 3.4 the treatment of collectives, in Section 3.5 the constrained POMDP synthesis problem, and, in the Sections 3.6 and 3.7, the extraction and verification of a strategy. We evaluate our approach in Section 4, discuss issues we encountered during modelling and synthesis in Section 5, and add concluding remarks in Section 6.

2 Preliminaries

Stochastic modelling is about describing uncertain real-world behaviour in terms of states and probabilistic actions producing transitions between these states. For stochastic reasoning (i.e., drawing conclusions about such behaviour), we use *probabilistic model checking*. This section introduces the *stochastic models*, *temporal logic*, and *tools* we employ for synthesis and verification.

Partially Observable Markov Decision Processes. Let $Dist(X)$ denote the set of discrete probability distributions over a set X , and $\mathbb{R}_{\geq 0}$ be the non-negative real numbers. Then, a POMDP [13] is given by

Definition 2.1. A POMDP is a tuple $M = (S, \bar{s}, A, P, R, \mathcal{O}, obs)$, where

- S is a set of states with $\bar{s} \in S$ being the initial state,
- A is a set of actions (or action labels),
- $P: S \times A \rightarrow Dist(S)$ is a (partial) probabilistic transition function,
- $R = (R_S, R_A)$ is a structure defining state and action rewards $R_S: S \rightarrow \mathbb{R}_{\geq 0}$ and $R_A: S \times A \rightarrow \mathbb{R}_{\geq 0}$,
- \mathcal{O} is a finite set of observations, and
- $obs: S \rightarrow \mathcal{O}$ is a labelling of states with observations.

Moreover, $A(s) = \{a \in A \mid P(s, a) \text{ is defined}\}$ describes the actions *available* in s . A *path* in M is defined as a finite or infinite sequence $\pi = s_0 \xrightarrow{a_0} s_1 \xrightarrow{a_1} \dots$ where $s_i \in S$, $a_i \in A(s_i)$, and $P(s_i, a_i)(s_{i+1}) > 0$ for all $i \in \mathbb{N}$. Let $last(\pi)$ be the last state of π . $FPaths_M$ and $IPaths_M$ denote all finite and infinite paths of M starting at state \bar{s} . Non-determinism in M is resolved through a *strategy* according to

Definition 2.2 (POMDP Strategy). A strategy for a POMDP M is a map $\sigma : FPaths_M \rightarrow Dist(A)$, where

- for any $\pi \in FPaths_M$, we have $\sigma(\pi)(a) > 0$ only if $a \in A(last(\pi))$, and
- for any path $\pi = s_0 \xrightarrow{a_0} s_1 \xrightarrow{a_1} \dots$ and $\pi' = s'_0 \xrightarrow{a'_0} s'_1 \xrightarrow{a'_1} \dots$ satisfying $obs(s_i) = obs(s'_i)$ and $a_i = a'_i$ for all i , we have $\sigma(\pi) = \sigma(\pi')$.

We call σ *memoryless* if σ 's choices only depend on the most recent state ($last(\pi)$), and *deterministic* if σ always selects an action with probability 1. Below, we consider memoryless deterministic strategies.

Probabilistic Linear Temporal Logic (PLTL). A POMDP M describes a stochastic process, such that every possible execution of that process corresponds to a *path* through M 's transition graph. To draw qualitative conclusions about M and its associated strategies, we express properties in linear temporal logic (LTL). An LTL formula ϕ over atomic propositions AP follows the grammar

$$\phi ::= ap \mid \neg\phi \mid \phi \wedge \phi \mid \mathbf{X}\phi \mid \phi \mathbf{U} \phi \quad (1)$$

where $ap \in AP$. In LTL, we make statements about M 's path structure and specify admissible sets of paths. Informally, $\mathbf{X}\phi$ describes that ϕ holds in the next state of a given path, and $\phi \mathbf{U} \psi$ describes that ϕ holds until ψ occurs, or globally, if ψ never occurs. We allow the abbreviations $\mathbf{F}\phi \equiv \top \mathbf{U} \phi$, describing that ϕ holds at some point on a path, and $\mathbf{G}\phi \equiv \neg\mathbf{F}\neg\phi$, describing that ϕ applies to the entire path.

To draw quantitative conclusions about M (or query probabilities and rewards), we use probabilistic LTL (PLTL), whose formulas ϕ are formed along (1) and by the two operators \mathbf{P} and \mathbf{R} :

- $\mathbf{P}_{[\min|\max] \sim p}=?[\psi]$ describes that the [minimum|maximum] probability of ψ (under all possible POMDP strategies) being valid is $\sim p$, and
- $\mathbf{R}_{[\min|\max] \sim r}^R[\psi]$ expresses that the [minimum|maximum] expected reward R associated with ψ (under all possible POMDP strategies) meets the bound $\sim r$,

where ψ is an LTL formula, $\sim \in \{<, \leq, =, \geq, >\}$, and $=?$ is used for queries. Given a timer t in M and that all actions in A increment t by 1, we allow $\mathbf{F}^{\sim T} \psi \equiv \mathbf{F}(t \sim T \wedge \psi)$. In LTL, $M \models \phi$ expresses that all paths of M from \bar{s} are permitted by ϕ , and, in PLTL, that a probability measure over M 's paths satisfies ϕ . For convenience, we use ϕ to refer to both, the expression and the region in S where it evaluates to true. LTL and PLTL's semantics are explained in detail in, for example, [1, p. 231 and Sec. 6.2].

The PRISM Model Checker can check $M \models \phi$ using exact and approximate algorithms [14]. It supports a variety of stochastic models and logics and has its own languages for modelling and for specifying properties. In PRISM, a reward structure R is used as a parameter in $\mathbf{R}^R[\cdot]$. For POMDPs, PRISM can synthesise strategies in the form of Definition 2.2.

A PRISM *model* consists of a series of *modules*, each defining a fraction of a state s using its own variables. *Modules* can synchronise their transitions by sharing labels from A , such that transitions in several modules using the same label can only switch in a state $s \in S$ if each transition is enabled in s . An example module with state variable x and command **increase** is given in Listing 1.

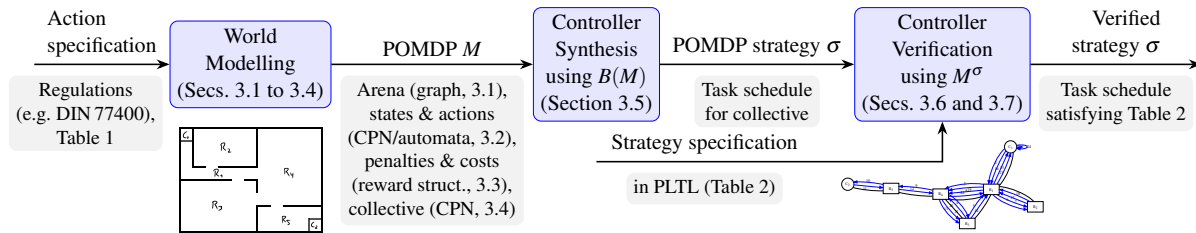


Figure 2: Overview of the proposed synthesis approach for robot collectives

```

1 module Example
2   x : [0..2] init 0; // state variable x with range {0,1,2} and initial value 0
3   [increase] x<2 -> (x'=x+1); // command increase increasing x by 1 if x < 2
4 endmodule

```

Listing 1: Example of a module in PRISM's guarded command language

Fixed-Grid Approximation in PRISM. When analysing a POMDP M , PRISM computes an approximate (finite-state) belief-MDP $B(M)$ [13], each *belief* being a probability distribution over the partially observable states (e.g., the possible room contamination). The size of $B(M)$'s state space, called *belief space* [10], is exponential in PRISM's grid-resolution parameter g controlling the approximation of the upper and lower bounds to be determined for $\mathbf{P} \mid \mathbf{R}^{\min|\max}$ -properties using $B(M)$.

3 Developing Controllers by Example of the Cleaning Scenario

In this section, we first state our synthesis problem and then describe our approach to strategy synthesis and verification as illustrated in Figure 2.

Problem Statement. Our aim to synthesise a collective controller is specified in the LTL property

$$\mathbf{G} \left(\underbrace{(\omega \rightarrow \mathbf{F}^{\leq T} (\omega \wedge \phi_r))}_{\text{reach task goal}} \wedge \underbrace{\mathbf{G}^{\leq T} \phi_s}_{\text{keep safe}} \right), \quad (2)$$

periodically achieve task safely (implied by our approach)

where ω is the *recurrence area* (including \bar{s} and acting as a task invariant), ϕ_r specifies an *invariant-narrowing condition*,¹ ϕ_s specifies *task safety*, and $T > 1$ is the *recurrence interval* (an upper cycle-time bound). Among the controllers satisfying (2), we look for an optimal (e.g., one minimising energy consumption) and robust (e.g., under partial observability of stochastic room contamination) one.

Overview of Controller Development. First, a spatio-temporal abstraction of the cleaning scenario is modelled using a coloured Petri net (CPN) for coordination modelling and finite automata for describing robot-local behaviour. These aspects are translated into a reward-enhanced POMDP M (Sections 3.1 to 3.3) in support of multiple robots (Section 3.4), which uses probabilistic actions to reduce the state count of a hypothetical detailed model. Then, a strategy σ is synthesised for M (Section 3.5), which is used to derive a *deterministic, non-probabilistic, and integer-valued* model M^σ (Section 3.6). Finally,

¹ ϕ_r only has methodological relevance. It could, for example, be used to develop an increasingly strong invariant ω .

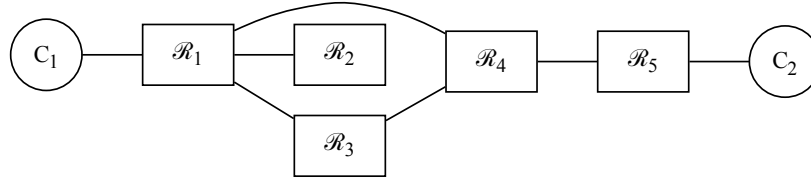


Figure 3: Example of a room plan graph

Table 1: Requirements of the cleaning scenario defining the **at** action implemented in three modules

Id.	Action Specification (Behavioural Requirement)	Impl. in Module
Ba	The robot either stays in the room it is currently in or moves to another room, whereby there must be an edge in the room plan graph between the current and next room.	cleaner
Bb	If the robot is on a charging station, its battery charge level is increased by the charging rate of the robot.	
Bc	If the robot is <i>not</i> on a charging station, its battery charge level is reduced by the robot's discharge rate.	
Da	The total contamination of each room increases by its contamination rate if there is no robot in that room.	contamination
Db	If the robot is in a room, the total contamination of that room is reset.	
Ta	The time counter is incremented by one.	time

M^σ , representing the high-level controller, is verified (Section 3.7) against strategy requirements that, due to current limitations in the formalisms and tools, cannot be checked directly during synthesis.

3.1 Spatio-temporal Abstraction

State Space. For the implementation of the problem (e.g., cleaning task), it is important to keep the number of states as small as possible. Therefore, large parts of the initial problem are abstracted.

Instead of a complete room plan with area assignment, the abstracted *environment* uses a graph that only contains the different rooms and charging stations. An example of such a graph for the room plan in Figure 1a can be seen in Figure 3. A pointer $B_i.x$, $i \in 0..k$, to a room or charging station in this graph is used to keep track of the position of robot B_i . The behaviour of the charging state $B_i.c$ of the robot's battery is described by a number of discrete charging levels and charge and discharge rates.

The total *contamination* is represented by a counter $\mathcal{R}_j.d$, $j \in 0..m$, whose maximum value is the contamination threshold $\mathcal{R}_j.threshold$. Since we want to avoid reaching a state with the contamination at this threshold, it is not necessary to model contamination beyond $\mathcal{R}_j.threshold$.

Actions and High-level Behaviour. Discrete values are used to model *time* as well, where the action **at**, as specified in Table 1 and described below, is performed at each discrete time step.

The CPN in Figure 4a provides a high-level description of the moves of the collective B across charging stations C and rooms \mathcal{R} (Figure 3). The abstract **at** action (black bar) expands to a range of concrete POMDP actions **at** $j_{B_1} \dots j_{B_k}$ with $j_{B_i} \in 0..m$. Whenever **at** is taken, any number of tokens (black dots, representing robots) on the places (grey circles, representing rooms and charging stations) can flow sim-

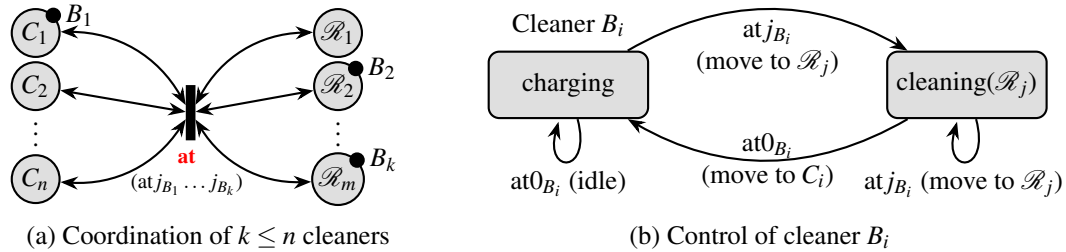


Figure 4: Cleaner coordination (a) as a CPN and local control (b) as a finite automaton

ultaneously, such that B_i can move from one place via **at** to an adjacent empty (possibly same) place.² Figure 4b outlines the control of a particular robot B_i . When composed (in parallel), as formalised in M by implicit constraints on the j -indices, simultaneous moves of several robots into a single place and jumps to non-adjacent places are prohibited by the coordination constraint in Figure 4a.³

3.2 Quantitative and Stochastic Abstraction

For the sake of simplicity, this section and the following will focus on a reduced problem with only one robot. The case of multiple robots will be reintroduced in Section 3.4.

As already mentioned, the PRISM-encoding of M is divided into three modules operating on three independent fragments of the state space S : The state of the robots, the room contamination, and time.

The cleaner module describes the behaviour of cleaning robot B_1 . An integer is used to model the robot position $B_1.x$. For this, each room and charging station is mapped to an integer bijectively. For example, the room graph in Figure 3 can be described by the following relation: $C_0 \rightarrow 0, \mathcal{R}_1 \rightarrow 1, \mathcal{R}_2 \rightarrow 3, \mathcal{R}_3 \rightarrow 4, \mathcal{R}_4 \rightarrow 5, \mathcal{R}_5 \rightarrow 6, C_2 \rightarrow 7$. The battery status $B_1.c$ is also described as an integer whose upper bound is the maximum charge $B_1.maxcharge$ of B_1 's battery, see Listing 2.

```

1 module cleaners
2   x : [0..m-1] init B1.start; // position of cleaner B1
3   c : [0..B1.maxcharge] init B1.ωchgthres; // battery status of B1
4   [at0] (x=0|x=1)
5     -> (x'=0) & (c=min(c+B1.chargerate, B1.maxcharge)); // charge B1
6   [at1] (x=0|x=1|x=2|x=3|x=4)
7     -> (x'=1) & (c=max(c-B1.dischargerate, 0)); // move to R1
8   ...
9 endmodule

```

Listing 2: A model fragment of the *cleaners* module highlighting its states and actions

For each charging station and each room there is a transition **atN** (where N is the integer assigned to the room), which models entering or staying in this room. The precondition for this transition is that the robot must already be in that room or a neighbouring room. If a robot enters or stays at a charging station, the charge increases by the charging rate; if a robot is in a room, the charge decreases by the discharge rate, see lines 5 and 7 respectively.

The contamination module describes the contamination status of \mathcal{R} . To reduce the number of states, contamination is modelled by booleans—the contamination flags $\mathcal{R}_j.d$, $j \in 1..m$ —rather than in-

²We assume for any initial state $\bar{s} \in S$ that no more than one robot is at a particular place.

³This construction reduces S and P of M in comparison with using alphabetised synchronous composition.

tegers. The probability $\mathcal{R}_j.pr$ of $\mathcal{R}_j.d$ getting true is used to model the state in which the contamination of the corresponding room has reached its threshold $\mathcal{R}_j.threshold$. If there is no robot in \mathcal{R}_j , we set $\mathcal{R}_j.d = \text{true}$ with probability $\mathcal{R}_j.pr$ inversely proportional to the contamination threshold $\mathcal{R}_j.threshold$. If a robot visits or stays in \mathcal{R}_j then $\mathcal{R}_j.d$ is set to `false`, see Listing 3.

```

1 module contamination // sequential stochastic contamination
2    $\mathcal{R}_1.d$  : boolean init false;  $\mathcal{R}_2.d$  : boolean init false;
3   ...
4   [at0] true -> 1 - ( $\sum_{i \in 1..m} \mathcal{R}_i.pr$ ): true
5     +  $\mathcal{R}_1.pr$ : ( $\mathcal{R}_1.d'=\text{true}$ ) +  $\mathcal{R}_2.pr$ : ( $\mathcal{R}_2.d'=\text{true}$ ) + ...; // probab. contam. all while charg.
6   [at1] true -> 1 - ( $\sum_{i \in 1..m \setminus 1} \mathcal{R}_i.pr$ ): ( $\mathcal{R}_1.d'=\text{false}$ )
7     +  $\mathcal{R}_2.pr$ : ( $\mathcal{R}_1.d'=\text{false}$ ) & ( $\mathcal{R}_2.d'=\text{true}$ ) + ...; // clean  $\mathcal{R}_1$  and probab. contam. other rooms
8   [at2] true -> 1 - ( $\sum_{i \in 1..m \setminus 2} \mathcal{R}_i.pr$ ): ( $\mathcal{R}_2.d'=\text{false}$ )
9     +  $\mathcal{R}_1.pr$ : ( $\mathcal{R}_2.d'=\text{false}$ ) & ( $\mathcal{R}_1.d'=\text{true}$ ) + ...; // clean  $\mathcal{R}_2$  and probab. contam. other rooms
10  ...
11 endmodule

```

Listing 3: A fragment of the `contamination` module (e.g. $\mathcal{R}_i.pr = 0.05$ for $i \in 1..m$)

The `time` module describes the progression of time and manages the switching to the error and final state (the model handles both the same). `time` also restricts the `atN` transitions so that they can only be used as long as the model is not in the error or final state. This is possible because a transition can only trigger if it can trigger in each module. Therefore, precondition in the `time` module can prevent a transition from triggering even though it is marked with `true` in the `cleaner` and `contamination` modules. The time is increased by one unit with each transition until it reaches T . At this point (due to the definition of `error_or_final`), only the `fin` transition can switch and the model ends in a loop, see Listing 4.

```

1 formula error_or_final = (c=0|!(t<T));
2 module time
3   t : [0..T] init 0;
4   [at0] !error_or_final -> (t'=min(t+1,T)); // charge
5   [at1] !error_or_final -> (t'=min(t+1,T)); // move to  $\mathcal{R}_1$ 
6   [fin] error_or_final -> (t'=min(t+1,T)); // finish cycle
7 endmodule

```

Listing 4: A fragment of the `time` module

3.3 Choice of the Reward Function

Four requirements, a valid strategy must satisfy, can be derived from Formula (2) and Table 1:

- FR At time T , all robots must be back in their initial location, so that the plan can be repeated.
- ω C At time T , the battery of a robot must not be lower than its threshold charge level.
- BC The battery of a robot must never be empty.
- CT The total contamination of any room must never exceed its contamination threshold.

When just focusing MDP verification rather than synthesis, it would be sufficient to describe these as PLTL constraints. However, PLTL constraints cannot be used as queries for synthesising *strategies*, since generating strategies through PRISM requires each path to be able to fulfil all constraints eventually.

Using constraints that are violated on some of M 's paths (e.g., if we require BC, any path leading to an empty battery eventually violates BC) will prevent PRISM from finding a reward-optimal strategy. This is a specific known limitation of the used formalism. Even though we cannot use PLTL constraints to encode all our requirements, the reward structure R can be used to prioritise selecting *strategies* that fulfil these requirements. The encoding of our requirements in R can be achieved by penalising states that do not fulfil some or all of the requirements, see Listing 5.

```

1 const a_lot = 10000000;
2 const a_bit = 10000;
3 rewards "penalties"
4   c=0:                                a_lot; // BC: battery empty
5   t=T & (x!=B1.start|c<B1.ωchgthres): a_lot; // FR: robot not at initial loc. at time T
6   R1.d=true:                            a_bit; // Room 1's contamination flag is set
7   R2.d=true:                            a_bit; // Room 2's contamination flag is set
8   ...
9 endrewards

```

Listing 5: An example of the reward structure for the *state penalties*

We previously found it ineffective to penalise the contamination flags the same as the constraints FR, ω C, and BC. Whereas the latter can be determined from M 's state, contamination flags only carry the probability of a requirement being violated. Hence, we apply lower penalties to the contamination flags. Further reward structures are used to model optimisation goals, such as energy consumption, see Listing 6a. However, the penalty for constraints is chosen such that it is not possible to offset the penalty of an invalid state by the reduced penalty for a less energy-consuming strategy.

```

1 rewards "energy consumption"
2   t < T: B1.maxcharge - c;
3 endrewards

```

(a) A fragment of the optimisation *rewards*

```

1 const a_lot = 10000000;
2 rewards "utilisation"
3   x=2 & t>=8 & t<10: a_lot;
4   x=2 & t>=12 & t<14: a_lot; ...
5 endrewards

```

(b) A fragment of room utilisation *rewards*

Listing 6: Fragments of the reward structure used for the cleaning scenario

Room Utilisation. As with the other requirements, a room utilisation profile to be respected by the cleaners (UT) can be softly specified using additional reward functions as shown in Listing 6b. However, UT as a safety property will later also be specified in PLTL and checked of the synthesised strategy.

3.4 Cooperation between Multiple Robots

To keep M simple, robots are not modelled as separate modules, but the state of the *cleaner* module is extended to include the positions of all robots (see Figure 4a). This simplification excludes all transitions from the model that would lead to conflicts in robot behaviour (e.g., the case where several robots clean the same room at the same time). Additionally, each robot has its own battery charge, see Listing 5.

```

1 x1 : [0..m] init B1.start;
2 x2 : [0..m] init B2.start;
3 ...
4 c1 : [0..B1.maxcharge] init B1.maxcharge;
5 c2 : [0..B2.maxcharge] init B2.maxcharge;
6 ...

```

Figure 5: The structure of the *cleaner* state

The `atN` actions for a single robot are now extended to `atN_N...` actions, which then model the simultaneous movement of k robots, as illustrated in Figure 4a and implemented in Listing 7.

```

1 [at0_1] !error & (x1=0|x1=1) & (x2=0|x2=1|x2=2|x2=3|x2=4) // charge B1 and move B2 to R1
2   -> (x1'=0) & (x2'=1)
3     & (c1'=min(c1+B1.chargerate,B1.maxcharge))
4     & (c2'=max(c2-B2.dischargerate,0));
5 [at1_2] !error & (x1=0|x1=1|x1=2|x1=3|x1=4) & (x2=1|x2=2) // move B1 to R1 and B2 to R2
6   -> (x1'=1) & (x2'=2)
7     & (c1'=max(c1-B1.dischargerate,0))
8     & (c2'=max(c2-B2.dischargerate,0));
9 ...

```

Listing 7: Two examples of `atN_N` actions

This solution increases the number of states per robot considerably, but the complexity of M is still within a practically verifiable range. Additionally, the reward structures that depend on the position and charge of a robot are adapted to include the position of all robots, as can be seen in Listing 8.

```

1 rewards "penalties"
2   c1=0: a_lot;
3   c2=0: a_lot;
4   ...
5   t=T & (x1!=B1.start|c1<B1.wchgthres): a_lot;
6   t=T & (x2!=B2.start|c2<B2.wchgthres): a_lot;
7   ...
8 endrewards
9
10 rewards "utilisation"
11   x1=2 & t>=8 & t<10: a_lot;
12   x2=2 & t>=8 & t<10: a_lot;
13   x1=2 & t>=12 & t<14: a_lot;
14   x2=2 & t>=12 & t<14: a_lot;
15   ...
16 endrewards

```

Listing 8: Reward structure for a collective

3.5 Synthesising Strategies (under Uncertainty) for the Cleaning Scenario

PRISM's POMDP strategy synthesis works under certain limitations. As indicated in Section 3.3, it is not possible to use $\mathbf{R}_{\min=?}^R[\psi]$ for synthesis if $\mathbf{P}_{\min=?}[\psi] < 1$, that is, if M contains ψ -violating paths under some strategy σ . Hence, we choose a ψ that defines a state that all paths converge at, and synthesise a strategy that minimises the total reward (since we model R using penalties) up to that point. A commonality of all paths is the flow of time, so the reachability reward-based synthesis query

$$\sum_{R \in \{\text{penalties, energy consumption, utilisation}\}} \mathbf{R}_{\min=?}^R[\mathbf{F}t = T] \quad (3)$$

uses a target state where time t is equal to some maximum time T .

Additionally, a mapping `obs` needs to be specified, which defines the observations of M that σ can use to make choices. In this case, σ cannot use the contamination flags to make its choices. If σ could consider the contamination flag, it would not need to account for the accumulative probability; σ could just check if a contamination flag is true and act accordingly. We can hide the contamination flags from σ by defining `obs` to just include the position and charge of the robot and the time, see the listing on the right.

```

1 observables
2   t,
3   x1, x2, ...,
4   c1, c2, ...
5 endobservables

```

PRISM allows the explicit generation of *deterministic* strategies. Such strategies are useful in this case, since, except for the final state, the model has no loops (i.e., time is always advancing). Because σ is deterministic, it can be thought of as a list of actions for each time step of the cleaning schedule, where the transition of each step of the strategy denotes the action of the robot at that time step within period T . Note that the observable environmental part of M is deterministic such that after applying σ , M^σ has exactly one path, hence, σ only depends on time t .

3.6 Creating an Induced Model from the Strategy

It is possible to create a cleaning schedule from the synthesised strategy σ . However, it is not yet possible to verify σ regarding the constraints listed in Section 3.3. This is because, up to this point, contamination was modelled in M only as a probabilistic factor. To verify the contamination constraint CT, below, we include a non-probabilistic contamination model in M' using counters to represent contamination.

Modelling the Contamination Value. To verify that the contamination value (modelled as a boolean sub-MDP of M) never actually reaches the thresholds $\mathcal{R}_j.threshold$, $j \in 1..m$, it is necessary to transform M into an MDP M' that accounts for the actual values $\mathcal{R}_j.d$. We accomplish this in M' by integer-valued contamination counters $\mathcal{R}_j.d$ (Listing 9) replacing the boolean variables $\mathcal{R}_j.d$ in M (Listing 3).

```

1 module contamination
2    $\mathcal{R}_1.d$  : [0.. $\mathcal{R}_1.threshold$ ] init 0;
3    $\mathcal{R}_2.d$  : [0.. $\mathcal{R}_2.threshold$ ] init 0;
4   ...
5   [at0_6] true -> ( $\mathcal{R}_1.d' = \min(\mathcal{R}_1.d + \mathcal{R}_1.contaminationrate, \mathcal{R}_1.threshold)$ )
6                 & ( $\mathcal{R}_2.d' = \min(\mathcal{R}_2.d + \mathcal{R}_2.contaminationrate, \mathcal{R}_2.threshold)$ ) & ...;
7   [at0_1] true -> ( $\mathcal{R}_1.d' = 0$ )
8                 & ( $\mathcal{R}_2.d' = \min(\mathcal{R}_2.d + \mathcal{R}_2.contaminationrate, \mathcal{R}_2.threshold)$ ) & ...;
9   [at0_2] true -> ( $\mathcal{R}_1.d' = \min(\mathcal{R}_1.d + \mathcal{R}_1.contaminationrate, \mathcal{R}_1.threshold)$ )
10                  & ( $\mathcal{R}_2.d' = 0$ ) & ...;
11  ...
12 endmodule

```

Listing 9: An example of the structure of the *contamination* module using discrete contamination values

Applying the Strategy. Apart from using contamination counters, our model does no longer contain probabilistic choices. Concretely, each probabilistic choice in M (branching to each possible selection of fully contaminated rooms, Listing 3) is replaced by an action in M' performing a simultaneous update of all contamination counters (Listing 9). We can use the generated strategy σ to derive the induced deterministic model M^σ from M' , which acts according to the strategy. This step is done by modifying the preconditions of the

`atN_N...` actions of the `time` module to only be able to trigger when that action is chosen at the same point in the strategy. If, for example, within σ , the `at0_1` action is only chosen in time steps 8 and 10, we modify the `time` module, see the listing on the right.

```

1 module time
2   ...
3   [at0_1] !error_or_final
4           & (t=8|t=10)
5           -> (t' = min(t+1, T))
6   ...
7 endmodule

```

Notes on the Relationship between M , M' , and M^σ . The state space of M' is significantly larger than the one of M as the latter contains intermediate contamination $\mathcal{R}_j.d$ up to $\mathcal{R}_j.d = \mathcal{R}_j.threshold$. The fact that \mathcal{R}_j gets contaminated in M corresponds to all shortest sequences of transitions with non-zero probability to a state where $\mathcal{R}_j.d = \text{true}$. The same fact in M' corresponds to all sequences of transitions leading to $\mathcal{R}_j.d = \mathcal{R}_j.threshold$. Hence, the time module in M^σ is a refinement of the time module in M and, due to synchronisation (via action labels), the resetting of contamination's (i.e., the cleaning) in M^σ is a refinement of the corresponding resets in M .

A property of M' preserving quantitative strategy correctness, that we left for future work, is to check whether the probabilities of the contamination flags set in M are greater than or equal to the hypothetical

Table 2: Requirements for validating the synthesised strategies (checks of M^σ by PRISM)

Id.	Strategy Specification (Behavioural Requirement)	... expressed in PLTL
FR	Cleaner B_i Finally Returns to its starting position.	$\bigwedge_{i \in [1..k]} \mathbf{P}_{\geq 1} [\mathbf{F}^{\leq T} B_i.x = B_i.start]$
ωR	Cleaner B_i has a final charge of at least $B_i.\omega chgthres$.	$\bigwedge_{i \in [1..k]} \mathbf{P}_{\leq 0} [\mathbf{F}^{\leq T} B_i.c < B_i.\omega chgthres]$
ωC	Contamin. of \mathcal{R}_i is finally less than $\mathcal{R}_i.\omega contthres$.	$\bigwedge_{i \in [1..m]} \mathbf{P}_{\leq 0} [\mathbf{F}^{\leq T} \mathcal{R}_i.d < \mathcal{R}_i.\omega contthres]$
BC	Battery charge of Cleaner B_i is never 0.	$\bigwedge_{i \in [1..k]} \mathbf{P}_{\leq 0} [\mathbf{F} B_i.c = 0]$
CT	Contamination of \mathcal{R}_i never exceeds \mathcal{R}_i 's threshold.	$\bigwedge_{i \in [1..m]} \mathbf{P}_{\leq 0} [\mathbf{F} \mathcal{R}_i.d \geq \mathcal{R}_i.threshold]$
UT	Room \mathcal{R}_i is not cleaned while occupied.	$\bigwedge_{i \in [1..m]} \bigwedge_{T \in util(\mathcal{R}_i)} \bigwedge_{j \in [1..k]} \mathbf{P}_{\leq 0} [\mathbf{F}^{\leq T} B_j.x = \mathcal{R}_i]$

probabilities of the corresponding counters in M' and, thus, M^σ , reaching their thresholds. This property, when true, expresses that the flags are a sound (i.e., conservative) quantitative abstraction of the counters.

3.7 Strategy Verification via Verifying the Induced Model

Now, we use M^σ to check *recurrence* and *safety* from Formula (2), that is, $\omega \rightarrow \mathbf{F}^{\leq T} \omega$ and $\mathbf{G}^{\leq T} \phi_s$.⁴ In particular, we check their decomposed translations into PLTL requirements⁵ listed in Table 2. The recurrence area ω is encoded by the state propositions in FR, ωR , and ωC , while safety ϕ_s is encoded by the state propositions in BC, CT, and UT. Note that the upper bound T of the recurrence interval is met by all paths in M^σ . $util(\mathcal{R}_i)$ is the set of time slots in which \mathcal{R}_i is utilised.

For checking $\omega \rightarrow \mathbf{F}^{\leq T} \omega$, we define ω to be a (not necessarily maximum) region in S from where σ can be applied and ω is revisited after T steps. The requirements for σ need to be true for every initial state in ω . FR, ωR , and ωC ensure that applying σ leads to a state within ω . To specify ω , we use thresholds for the battery charge of robots ($B_i.c$ for every robot B_i) and the contamination of rooms ($\mathcal{R}_i.\omega contthres$ for every room \mathcal{R}_i). ω then characterises every state of M^σ where the battery charge and room contamination are within these thresholds and all robots are on their starting position. Recurrence can even be checked more easily for M^σ by selecting the worst state in ω , which is the state where every value lies exactly at the thresholds, and verifying the requirements in Table 2 for this state.

4 Experimental Evaluation

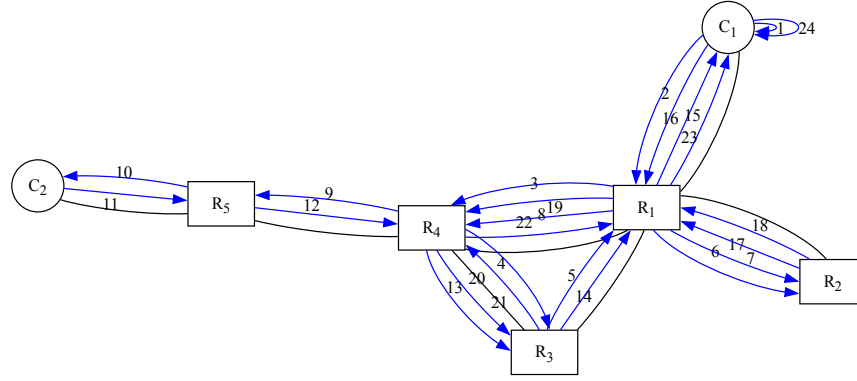
Our experimental evaluation addresses two research questions (RQs).

4.1 RQ1: Can we synthesise reasonable strategies for multiple robots?

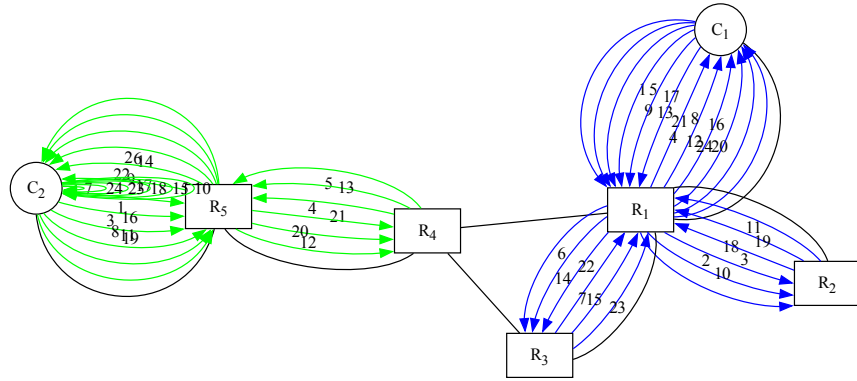
In the following, an instance of the example model with only one robot is considered first. The contamination rate is the same for all rooms, except that $\mathcal{R}_5.d$ has a threshold value $\mathcal{R}_5.threshold$ of 24 (based on a contamination rate of 1 h^{-1}), which is twice as high, whereas all other rooms have a threshold value of 12. We identified ω manually by examining the generated strategy. Using the method described in Section 3, a strategy was generated that meets all the requirements. This strategy is visualised in Figure 6a. Each action is shown with a blue arrow, at which the time step in which the action is to be executed is annotated. To develop a strategy for two robots, the battery charge was halved to keep the

⁴For the sake of simplicity of the example, we use $\phi_r \equiv \top$ and can omit $\omega \rightarrow \mathbf{F}^{\leq T} \phi_r$.

⁵All properties are expressed in quasi-LTL, that is, ACTL* allowing only one universal quantifier at the outermost level.



(a) Strategy for one robot



(b) Strategy for two robots (blue and green directed arcs)

t	0	1	2	3	4	5	6	7	8	9	10	11	12	13	14	15	...	24
B ₁	C₁	R₁	R₂	R₁	C₁	R₁	R₃	R₁	C₁	R₁	R₂	R₁	C₁	R₁	R₃	R₁	...	C₁
B ₂	C₂	R₁	C₂	R₅	R₄	R₅	C₂	idle	R₅	C₂	idle	R₅	R₄	R₅	C₂	idle	...	C₂

(c) Execution of a 24h model cycle using the strategy in Figure 6b; (sub-)cycles indicated in bold

Figure 6: Synthesised strategies. Nodes represent charging stations and rooms; undirected arcs indicate room connections (doors); edge labels specify the execution order of particular **at** actions.

model less complex. The corresponding strategy can be seen in Figure 6b. This result turns out to be a *partition-based patrolling strategy*, considered effective under random disturbance [15, 143].

4.2 RQ2: How do model parameters influence the synthesis of recurrent strategies?

We evaluate the model using *a_bit*, $\mathcal{R}_i.pr$, and the fixed-grid resolution *g* as parameters. Figure 7 visualises the result using these parameters on a simplified model, which only contains one robot and omits room \mathcal{R}_5 and charger C_2 . When building σ , we set $\mathcal{R}_i.pr = cumulative_probability/|\mathcal{R}|$. The generated strategies were verified by iteratively assuming ω -thresholds (Table 2) from a set chosen appropriately.

Figure 7 contains four plots for resolutions $g = 1..4$. Correct non-recurrent strategies are represented by a blue dot, correct recurrent strategies by a green dot, and incorrect strategies in red.

We deemed the simplification of the model necessary to allow a timely execution of the test series, which contained 400 experiments in total (100 for each grid resolution). Detailed information about the

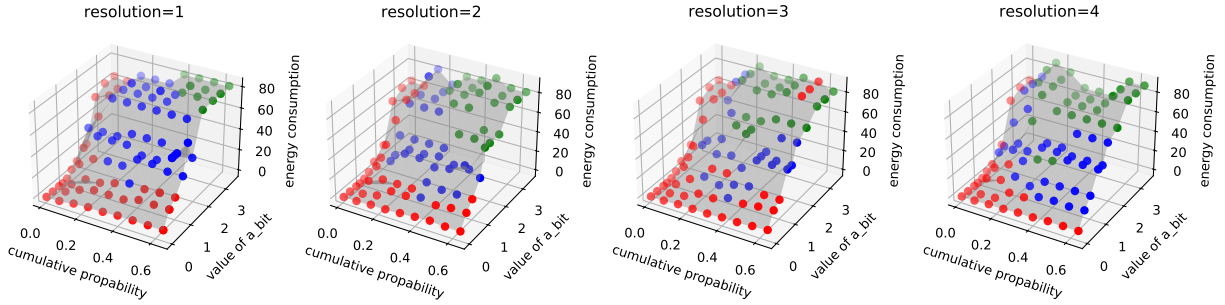


Figure 7: Parameterised evaluation. Non-recurrent strategies are marked in blue, recurrent strategies in green. The scale for a_bit is logarithmic.

time of the evaluation is shared at the end of the section.

As expected, a smaller cumulative contamination probability leads the strategy to de-prioritise cleaning the rooms regularly, since the probability of them being contaminated stays low. This, at some point, causes the strategy to not satisfy the recurrence criteria. Similarly, a lower value of a_bit causes the strategy to prioritise saving battery over resetting the contamination flags, which reduces the energy consumption significantly, but at some point at the cost of strategy correctness.

In the evaluation, the optimal strategy per grid resolution uses less or equal energy with a larger grid resolution (84, 64, 64, and 36 for g of 1, 2, 3, and 4, respectively). There is also a difference in the number of distinct strategies that are generated between the different g , where the experiment with a resolution of 4 generates more unique strategies than the experiments with lower grid resolutions, where many parameters lead to the same generated strategy.

Finally, we can observe distinct areas of incorrect, non-recurrent and recurrent strategies that depend on these parameters, where the optimal recurrent strategy lies on the border between recurrent and non-recurrent strategies. While the states in ω are ordered for the choice of a worst case, the border area is at best an approximation of a Pareto front, the non-convex reward function defined by R combined with the belief-MDP approximation $B(M)$ may lead to optimal strategies remaining hidden from the search.

Beyond the reward structure $R^{utilisation}$ used for strategy pre-selection, checking the PLTL safety property UT (Table 2) ensures that the finally chosen strategy only cleans outside the room utilisation schedule (Figure 1b).

Some Key Data. The experiments were conducted on an AMD FX(tm)-8350 Eight-Core Processor with 32 GiB of RAM running Ubuntu 22.04.4 LTS. However, PRISM was restricted to one core and 12 GiB of RAM. The reduced model in Section 4.2 contains 4879 states and 35014 transitions, while the reduced model M^σ contains 23 states and 23 transitions. The verification consists of 13 PLTL formulas containing 25 propositions. We ran the experiments with parameters of $m = 4$, $\mathcal{R}_i.pr = 0.02, 0.04, \dots, 0.16$ and $a_bit = 1, 3, 6, 10, 17, 32, 100, 316, 1000, 3162$. The *cumulative probability* can be derived from \mathcal{R}_i : $\sum_{i=1, \dots, m} \mathcal{R}_i.pr = 0.08, 0.16, \dots, 0.64$. The strategy synthesis took about 5, 16, 60, and 200 seconds for a grid resolution of 1, 2, 3, and 4, respectively, while the verification took about one second for a given ω . Evaluating the entire test series took about 8 hours sequentially, although this process could be easily parallelised.

5 Discussion

Selecting the Recurrence Area ω . When evaluating the strategy, ω was chosen either by examining the strategy manually (Figure 6c) or by verifying a list of probable ω s. Further work may focus on finding probable ω s from the room layout, and generating strategies which fulfil these ω s.

Complexity of the Cleaning Scenario. For the evaluation, we considered a rather simple room layout. The performance of the above described method may be different with larger room graphs, more complex room layouts, a larger number of robots, and tighter restrictions on battery charge and room utilisation.

Moreover, our model allows us to find strategies that operate with a varying number of robots. Given that some robots remain idling all the time, our optimal synthesis could also be used to find the smallest subset $B_{\min} \subseteq B$ or minimal number $k_{\min} \leq k$ of robots for an optimal task performance.

The complexity of the model is heavily dependant on the number of rooms, the maximum time T , and the maximum charge of the robots. Following the comprehensive scheme in Section 4.2, we were able to calculate a 12-hour ($T = 12$) cleaning schedule for 3 robots with 11 rooms and a maximum charge of 6 in 15 hours. The corresponding belief-MDP $B(M)$ contains ≈ 690 k states and ≈ 11.8 m transitions.

Adjusting Grid-Resolution vs. Filtering Strategies. For industry-size POMDPs, a high resolution g can lead to an impractically high computational effort when solving the mostly NP-hard approximate analysis (i.e., verification, synthesis) problems. Hence, our approach is to keep g just fine enough to find some (not necessarily globally optimal) strategy σ and verify more nuanced properties of the quasi-MDP⁶ M^σ derived from M by applying σ . In M^σ , verification is simpler (no belief-MDP $B(M)$ is computed), also the strategy (integrated in M^σ) can directly observe the outcome of each action and does not have to memorise a finite observation history. Despite the expansion of $\mathcal{R}_{i,d}$ to integers, M^σ 's state space is expected to be smaller than $B(M)$'s state space for the applied values of g .

Parameter Selection. For the evaluation in Section 4.2, a set of values for the parameters *a_bit* and the *contamination probability* was chosen. Via g (Section 2), we reduced the resolution of the fixed grid (i.e., a wider grid width) to limit the number of states in the belief space approximation $B(M)$. However, our findings in Section 4.2 suggest that increasing the resolution, while keeping the cumulative contamination probability around 40 % and the value of *a_bit* around 300 leads to the synthesis of better strategies. However, these values may not be universally favourable for any room layout, and it may be possible to synthesise better strategies using a different set of parameters. Further work may focus on better ways of parameter selection.

Generalisation to Other Applications. The running example in our case study focuses on a cleaning robot collective. However, we think that our approach and model can be transferred rather straightforwardly to other spatio-temporal settings with recurrent tasks, for example,

- firefighting drone collectives tasked with repetitive sector-wise fire detection and water distribution and with partially observable quantities such as ground temperature and extinction level;
- geriatric care robot collectives tasked with recurrent monitoring and care-taking tasks (e.g., medication supply) with patient satisfaction and health status being partially observable;
- general patrolling collectives tasked with monitoring or supervising specific environments [15].

⁶non-probabilistic, deterministic, with full observability

6 Conclusion

We proposed an approach using weighted, partially observable stochastic models (i.e., reward-enhanced POMDPs) and strategy synthesis for optimally coordinating tasked robot collectives while providing recurrence and safety guarantees on the resulting strategies under uncertainty. Along with that, we discussed guidance on POMDP modelling and strategy synthesis. We focused on a cleaning robot scenario for public buildings, such as schools. Our notion of *correctness* combines (i) safe recurrence (e.g., repetitively accomplish the cleaning task while avoiding to collect penalties), (ii) robustness (e.g., correctness under worst-case contamination), and (iii) optimality (e.g., minimal energy consumption).

For scaling up strategy synthesis to scenarios beyond what can easily be tackled by stochastic game-based synthesis, we addressed the key challenge [6] of reducing the state space and the transition relation of a naïve model via partial observability (hiding details of stochastic room contamination) and by employing simultaneous composition (for robot movement). PRISM’s grid-based POMDP approximation allowed us to adjust the level of detail of the belief space to synthesise strategies more efficiently. Furthermore, we softly encode the strategy search space using penalties and optimisation rewards and can, thus, shift the verification of more complicated properties to a later stage working with an unweighted and non-probabilistic behavioural model, again using a more detailed, numerical state and action space. However, decoupling synthesis from verification can require time-consuming experiments (Section 4.2) to identify regions of the parameter space for ensuring the existence of good recurrent strategies.

In future work, we will improve finding ω ensuring the existence of correct strategies (i.e., green dots in Figure 7). Ideally, we avoid defining ω explicitly (e.g., by hiding time). In a larger example, we want to allow invariant-narrowing with ϕ_r and observable stochasticity in the environment, such that σ can depend on arbitrary variables. The reset of the contamination flag on a room visit (Db) could be refined by a decontamination rate in M^σ . Moreover, we aim to use multi-objective queries to include further criteria (e.g., minimal contamination) for Pareto-optimal strategy choice. While PRISM imposes some limits on the combination of queries and constraints, we will need to see how we can use tools such as EVOCHECKER (as, e.g., used in [17]) for POMDPs. Also, we can further reduce the action set by taking into account trajectory intersections in the simultaneous movements (cf. Figure 4a). Finally, we want to connect the synthesis pipeline with code generation, such as demonstrated in our previous work [5].

References

- [1] Christel Baier & Joost-Pieter Katoen (2008): *Principles of Model Checking*. MIT Press.
- [2] Davide Basile, Maurice H. ter Beek & Axel Legay (2020): *Strategy Synthesis for Autonomous Driving in a Moving Block Railway System with UPPAAL Stratego*. In: *FORTE, LNPSE* 12136, Springer, pp. 3–21, doi:10.1007/978-3-030-50086-3_1.
- [3] DIN (2015): *DIN 77400: Reinigungsdienstleistungen - Schulgebäude - Anforderungen an die Reinigung*. Standard, DIN. Available at <https://www.dinmedia.de/de/norm/din-77400/237208488>.
- [4] Ruben Giaquinta, Ruth Hoffmann, Murray Ireland, Alice Miller & Gethin Norman (2018): *Strategy Synthesis for Autonomous Agents Using PRISM*, p. 220–236. Springer, doi:10.1007/978-3-319-77935-5_16.
- [5] Mario Gleirscher, Radu Calinescu, James Douthwaite, Benjamin Lesage, Colin Paterson, Jonathan Aitken, Robert Alexander & James Law (2022): *Verified Synthesis of Optimal Safety Controllers for Human-Robot Collaboration*. *Sci. Comput. Program.* 218, p. 102809, doi:10.1016/j.scico.2022.102809. arXiv:2106.06604.
- [6] Mario Gleirscher, Jaco van de Pol & James Woodcock (2023): *A Manifesto for Applicable Formal Methods*. *Softw. Syst. Model.* 22, pp. 1737–1749, doi:10.1007/s10270-023-01124-2. arXiv:2112.12758.

- [7] Rong Gu, Peter G. Jensen, Cristina Seceleanu, Eduard Enoiu & Kristina Lundqvist (2022): *Correctness-guaranteed strategy synthesis and compression for multi-agent autonomous systems*. *Sci. Comput. Program.* 224, p. 102894, doi:10.1016/j.scico.2022.102894.
- [8] Umweltbundesamt (Hrsg.) (2008): *Leitfaden für die Innenraumhygiene in Schulgebäuden*. Available at <https://www.umweltbundesamt.de/sites/default/files/medien/publikation/long/3689.pdf>.
- [9] Bruno Lacerda, David Parker & Nick Hawes (2017): *Multi-Objective Policy Generation for Mobile Robots Under Probabilistic Time-Bounded Guarantees*. In: *Automated Planning and Scheduling (ICAPS), 27th Int. Conf.*, pp. 504–512, doi:10.1609/icaps.v27i1.13865.
- [10] William S. Lovejoy (1991): *Computationally Feasible Bounds for Partially Observed Markov Decision Processes*. *Oper. Res.* 39(1), p. 162–175, doi:10.1287/opre.39.1.162.
- [11] Owen Macindoe, Leslie Pack Kaelbling & Tomás Lozano-Pérez (2012): *POMCoP: Belief Space Planning for Sidekicks in Cooperative Games*. In: *AIIDE*, The AAAI Press, pp. 38–43, doi:10.1609/aiide.v8i1.12510.
- [12] Pierre El Mqirmi, Francesco Belardinelli & Borja G. León (2021): *An Abstraction-based Method to Check Multi-Agent Deep Reinforcement-Learning Behaviors*. In: *AAMAS*, pp. 474–482, doi:10.5555/3463952.3464012. arXiv:2102.01434.
- [13] Gethin Norman, David Parker & Xueyi Zou (2017): *Verification and control of partially observable probabilistic systems*. *Real-Time Systems* 53(3), p. 354–402, doi:10.1007/s11241-017-9269-4.
- [14] Dave Parker, Gethin Norman & Marta Kwiatkowska (2024): *PRISM Model Checker*. Available at <http://www.prismmodelchecker.org/manual/>.
- [15] David Portugal & Rui Rocha (2011): *A Survey on Multi-robot Patrolling Algorithms*, pp. 139–146. Springer, doi:10.1007/978-3-642-19170-1_15.
- [16] Antony Thomas, Fulvio Mastrogiovanni & Marco Baglietto (2021): *MPTP: Motion-planning-aware task planning for navigation in belief space*. *Robot. Auton. Syst.* 141, p. 103786, doi:10.1016/j.robot.2021.103786.
- [17] Grice Vázquez, Radu Calinescu & Javier Cámara (2022): *Scheduling of Missions with Constrained Tasks for Heterogeneous Robot Systems*. In: *Proceedings Fourth International Workshop on Formal Methods for Autonomous Systems (FMAS) and Fourth International Workshop on Automated and verifiable Software sYstem DEvelopment (ASYDE), EPTCS 371*, Open Publishing Association, pp. 156–174, doi:10.4204/eptcs.371.11. arXiv:2209.14040.